Available online at www.sciencedirect.com
SCIENCE DIRECT®
Journal of Power Sources 131 (2004) 217–223
JOURNAL OF POWER SOURCES
www.elsevier.com/locate/jpowsour

Bi- and tri-metallic Pt-based anode catalysts for direct ethanol fuel cells

W.J. Zhou [a], W.Z. Li [a], S.Q. Song [a], Z.H. Zhou [a], L.H. Jiang [a], G.Q. Sun [a], Q. Xin [a,*], K. Poulianitis [b], S. Kontou [b], P. Tsiakaras [b]

[a] *Dalian Institute of Chemical Physics, China Academy of Science, Dalian 116023, PR China*
[b] *Department of Mechanical and Industrial Engineering, University of Thessalia, Pedion Areos, 383 34 Volos, Greece*

Received 30 September 2003; accepted 16 December 2003

Abstract

In the present work, several Pt-based anode catalysts supported on activated carbon XC-72R were prepared by using a novel method, characterized and tested. XRD analysis and TEM images indicated that all of anode catalysts consist of uniform nanosized particles with sharp distribution and that the Pt lattice parameter becomes shorter with the addition of Ru and Pd and bigger with the addition of Sn and W. Cyclic voltammetry (CV) measurements and single direct ethanol fuel cell (DEFC) tests jointly showed that Sn, Ru and W can enhance ethanol electro-oxidation activity of Pt in the following order: $Pt_1Sn_1/C > Pt_1Ru_1/C > Pt_1W_1/C > Pt_1Pd_1/C > Pt/C$. The Pt_1Ru_1/C catalyst was modified with Mo, W and Sn, respectively. It was found that the DEFCs performances were improved with these modified Pt_1Ru_1/C catalysts as anode catalysts. This distinct DEFC performance behavior is attributed to the so-called bifunctional mechanism and to the electronic interaction between Pt and additives.

Keywords: Direct ethanol fuel cells; Bi-metallic and tri-metallic catalysts; Ethanol energy

1. Introduction

The low-temperature fuel cells that can run directly on liquid fuels such as methanol and ethanol and so on are gaining more and more interest especially for the large potential market for fuel cell vehicle applications [1]. Operating on liquid fuel would assist in rapid introduction of fuel cell technology into commercial markets, because it will greatly simplify the on-board system and reduce the infrastructure needed to supply fuel to passenger cars and commercial fleets. Compared to H_2/O_2 PEMFCs, the direct alcohol PEMFCs are more compact without heavy and bulky fuel reformer and can be especially applied to power electric vehicles. Liquid fuels, such as low-molecular weight alcohols, featuring higher volumetric and gravimetric energy densities and better energy efficiency, can be easily handled, stored and transported compared to the gas fuels such as pure hydrogen. Among these low-molecular weight alcohols, methanol currently appears to be the particularly favorite fuel for these direct electro-oxidation fuel cells and fuel cell-driven automobiles [2–4], and in particular the direct methanol fuel cells (DMFCs) research has been given more attention and investments in the past decade. However, there are still open questions related to DMFCs such as serious methanol crossover from anode side to cathode side. Another disadvantage of methanol is that it is volatile and relatively toxic to eyes. Ethanol has a similar molecular structure to methanol and is relatively reactive. Moreover, ethanol is a green fuel and readily produced from renewable resources. Ethanol is rich of hydrogen and can be used indirectly to prepare H_2 for H_2/air PEMFCs. Therefore, ethanol is attractive to fuel cells whenever it is directly used to direct ethanol fuel cells (DEFCs) or indirectly used to fuel H_2/air PEMFCs by reforming. The electrochemical oxidation of ethanol has been the subject of a large number of recent investigations. In most of previous studies, spectroscopic techniques such as IR, MS and GC are the most common tools used to identify the products and intermediates of ethanol electro-oxidation. The established major products include CO_2, acetaldehyde and acetic acid, and it is reported that methane and ethane have been also detected [5]. Surface adsorbed CO is still identified as the leading intermediate in ethanol electro-oxidation as in the methanol electro-oxidation. Other surface intermediates include various C_1 and C_2 small molecular such as ethoxy and acetyl [5,6].

* Corresponding author. Tel.: +86-411-4379710; fax: +86-411-4379710.
E-mail address: xinqin@dicp.ac.cn (Q. Xin).

0378-7753/$ – see front matter © 2004 Elsevier B.V. All rights reserved.
doi:10.1016/j.jpowsour.2003.12.040

It is reported that ethanol electro-oxidation contains several reaction pathways [7]. Carbon dioxide is the favorite product and other products and by-products such as acetaldehyde and acetic acid will inevitably decrease the fuel efficiency. The electro-oxidative removal of CO-like intermediates and the cleavage of C–C bond are the two main obstacles and rate-determining steps. Although either increasing reaction temperature or adopting more active electrocatalysts can enhance the ethanol electrochemical reaction activity, increasing reaction temperature is not, at least at present, the primary choice because the present perfluosulfonic-based polymer electrolyte membranes dehydrate at higher operation temperatures, which results in the intrinsic impedance increase and consequently deteriorate the fuel cell performance [8]. It is clear that ethanol electro-oxidation involves more intermediates and products than that of methanol, and thus more active electrocatalysts are needed to promote ethanol electro-oxidation at lower temperatures. The nature and structure of the eletrocatalysts play a crucial role in ethanol adsorption and electro-oxidation, and the catalyst preparation procedure affects the catalyst nature and structure, especially the various interactions between the different elements.

The present work reports several carbon-supported Pt-based bimetallic and ternary metallic catalytic activities for ethanol electro-oxidation. These catalysts were prepared according to a novel and convenient method and characterized by X-ray diffraction (XRD) and transmission electron microscope (TEM). Cyclic voltammetry (CV) measurements and single DEFC tests were used to evaluate the electrocatalytic activities for ethanol electro-oxidation.

2. Experimental

All the carbon-supported Pt-based catalysts were prepared according to the method mentioned in the literature [9]. As described briefly, the precursors of Pt and other metals were added dropwise to the carbon slurry, which was dispersed in the mixture solution of water and ethylene glycol. After being kept at 130 °C for 2 h with a pH of 13, the mixture was filtered, washed with copious deionized water and dried at 70 °C for 12 h. The atomic ratio of Pt to other metallic elements of these catalysts was 1/1 or 1/1/1, and the Pt loading of every anode catalyst was always 20.0 wt.%. Powder X-ray diffraction (XRD) patterns of all samples were obtained with a Regaku X-3000 X-ray powder diffractometer. The scan range was from 20° to 90° with a scan rate of 4°/min. The range from 60° to 75° was scanned finely at a rate of 1.0°/min to obtain the Pt (2 2 0) reflection. Catalyst samples were also examined using the JEOL JEM-2011 electron microscopes operated at 100 kV to get TEM patterns. More than 300 particles were calculated to get the integrated information about every Pt-based catalyst.

The cyclic voltammetry spectra were recorded using the potentiostat/galvanostat (EG&G Model 273A) and experiments were carried out in a solution containing 0.5 M H_2SO_4 and 1.0 M ethanol at room temperature. The membrane electrode assembles (MEAs) were fabricated according to the method described in literature [10,11]. Commercial catalyst 20.0 wt.% Pt/C (Johnson Matthey Co.) was consistently used as cathode catalyst for oxygen cathodic reduction. The catalyst ink was prepared by directly mixing a suspension of Nafion® ionomer ethanol solution with catalyst powder in an ultrasonic bath. Then, the resulting paste was spread onto carbon paper backing layer to prepare the electrode. The Pt loadings of cathode and anode are 1.0 and 1.3 mg/cm^2, respectively. The MEA was manufactured by pressing the electrodes onto either side of Nafion®-115 membrane at 130 °C for 90 s. The MEA was loaded into an in-house single-cell test fixture. Aqueous solutions of ethanol and un-humidified oxygen were fed to the cell. The operating temperature of the cell was kept at 90 °C. Under the same conditions, the single direct ethanol fuel cell (DEFC) with Pt_1Ru_1 and Pt_1Sn_1 as anode catalysts respectively were also investigated as half-cells, in which the cathode was fed by the humidified hydrogen and used as counter electrode and reference electrode. The scan rate was 2 mV/s and the anode was still fed by ethanol solution.

3. Results and discussion

XRD and TEM results: The XRD patterns of various carbon-supported binary and ternary metal catalysts were given in Fig. 1. Exhibited in Fig. 2 are (2 2 0) planes of Pt/C and carbon-supported Pt-M catalysts. The diffraction peak at 20–25° observed in all the diffraction patterns of the carbon-supported catalysts is attributed to the (0 0 2) plane of the hexagonal structure of Vulcan XC-72 carbon. All the carbon-supported catalysts synthesized with the novel method only show the Pt (fcc) crystalline structure. The (2 2 0) reflections of Pt-based catalysts were used to calculate the average particle size according to the Scherrer formula

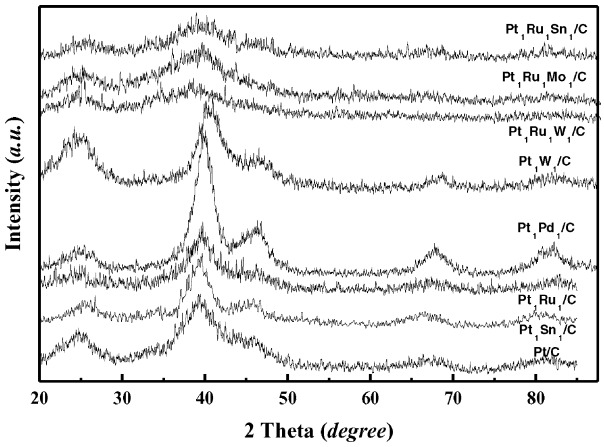

Fig. 1. XRD patterns of carbon-supported bi- and tri-metallic Pt-based catalysts.

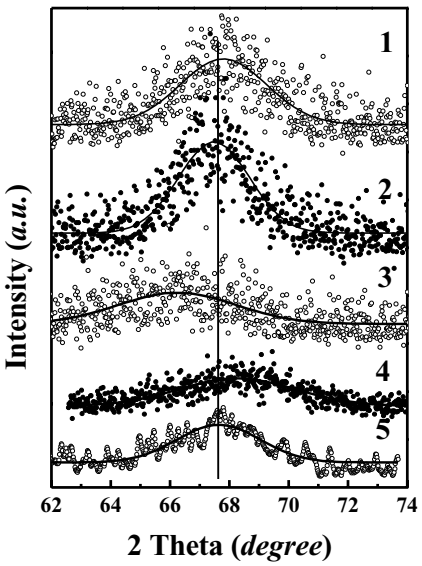

Fig. 2. XRD patterns of different carbon-supported Pt-based bimetallic electrocatalysts. (1) Pt_1Pd_1/C; (2) Pt_1W_1/C; (3) Pt_1Sn_1/C; (4) Pt_1Ru_1/C; (5) Pt/C.

[12]. There are obvious differences between the bimetallic catalysts in the noble metal particle size and the shift of the reflections peak of (2 2 0) plane compared to that of Pt/C catalyst, while no obvious differences among those tri-metallic catalysts from the XRD results. The Pt_1Ru_1/C catalyst had smaller particle diameter compared to that of Pt/C, and the mean particle size of Pt_1Ru_1/C and Pt/C were 1.8 and 2.6 nm calculated from the (2 2 0) reflection parameters. The metal particle size was about 3.2 nm for Pt_1W_1/C, 2.8 nm for Pt_1Pd_1/C and 1.9 nm for Pt_1Sn_1/C, respectively. The lattice parameter of PtM catalyst fcc place was 3.9223 Å for Pt_1W_1/C, 3.9064 Å for Pt_1Pd_1/C and 3.9873 Å for Pt_1Sn_1/C, respectively. The lattice parameter of the fcc Pt_1Ru_1/C was 3.8830 Å, while the lattice parameter of 20% Pt/C catalyst synthesized by the same method was 3.9162 Å. The shift of (2 2 0) plane and the difference of lattice parameters indicate that there were interactions between Pt and other addictives such as W, Ru, Pd and Sn. The interactions between Pt and Ru, Pd were different from the interaction between Pt and Sn (W). The addition of Sn and W extended the Pt lattice parameters, while the addition of Ru and Pd resulted in the decrease of Pt lattice parameters.

It was observed that metal particles of all Pt-based catalysts were very uniform from the TEM results. The mean particle size of Pt_1Sn_1/C catalyst was about 2.4 nm with a sharp size distribution. Other three Pt_1Ru_1-based catalysts (namely $Pt_1Ru_1W_1$/C, $Pt_1Ru_1Mo_1$/C, $Pt_1Ru_1Sn_1$/C,) had similar particle size. The samples of Pt_1W_1/C and Pt_1Pd_1/C had mean particle sizes of 3.4 and 3.0 nm, respectively. The mean particle sizes according to the TEM and XRD results were identical for these Pt-based catalysts. The TEM and XRD results showed that nanometer-sized noble catalysts can be easily prepared by the method adopted here and the method was suitable to prepare supported Pt-based catalysts in the presence of higher metal loadings.

CV and single fuel cell test results: The Fig. 3 shows the results of CV experiments with different carbon-supported Pt and PtM catalysts. There are two oxidation peaks when the ethanol CV is carried out on the Pt/C catalyst. The first one appears at around 0.76 V (versus SCE) and the second one appears at higher potential. Only the first oxidation peak is reported in the present work and the applied upper potential is not allowed to exceed 1.0 V versus SCE to prevent the assistant metals to dissolve out. The addition of the second metal to Pt results in the negative shift of the first ethanol electro-oxidation peak. The first oxidation peak on Pt_1Ru_1/C appears at the most negative potential, at around 0.53 V (versus SCE), and the peak potential is about 0.23 V lower than that on Pt/C catalyst. The first electro-oxidation peak of ethanol on Pt_1Pd_1/C is around 0.65 V (versus SCE), higher than that on Pt_1Ru_1/C. The current density at the first peak of the ethanol electro-oxidation on Pt_1Ru_1/C is higher than that on Pt_1Pd_1/C, but less than these on Pt_1Sn_1/C, Pt_1W_1/C and Pt/C, respectively. The Pt_1Sn_1/C catalyst has the highest electrocatalytic activity towards ethanol oxidation in terms of first peak current density, but also has a higher overpotential (0.71 versus

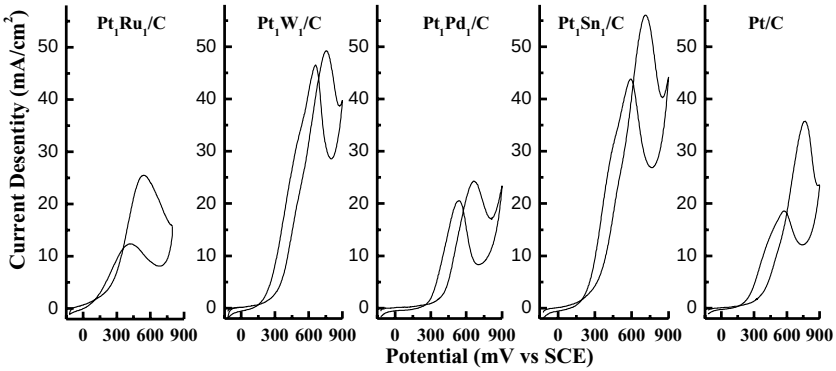

Fig. 3. The CV results of different anode catalysts for ethanol electro-oxidation. Operation temperature: 25 °C. Scan rate: 10 mV/s. Electrolyte: 1.0 M EtOH + 0.5 M H_2SO_4.

SCE). Pt_1W_1/C catalyst also exhibits a higher current density than those of Pt/C and Pt_1Ru_1/C and Pt_1Pd_1/C, but has a similar overpential (0.75 versus SCE) to Pt/C. It seems that Pt_1Sn_1/C is the best electrocatalyst for ethanol oxidation from the point of current density. Pt_1Ru_1/C has the lowest overpotential to ethanol electro-oxidation among the above electrocatalysts, which indicates that Pt_1Ru_1/C is also a promising catalyst for ethanol electro-oxidation.

The above five catalysts were evaluated as anode catalysts for ethanol electro-oxidation by the single DEFC test. The single fuel cell test is not the optimal tool for electrocatalyst evaluation, because there are so many influencing factors. But the performances of single fuel cells with different anode catalysts are greatly different when other factors such as electrolyte, cathode catalyst are defined. On the other hand, from a practical point of view every potential electrocatalyst should be ultimately investigated in fuel cells. Fig. 4 exhibits the performance difference between the single fuel cells with different anode catalysts operated at 90 °C. When Pt/C is used as anode catalyst for ethanol, the performance of single fuel cell is poor. The open circuit voltage (OCV) is only around 0.55 V, far less than the standard electromotive force (1.145 V) [7], which is mainly attributed to poor catalytic activity to ethanol electro-oxidation and ethanol crossover from anode to cathode. The maximum output power density is only 10.8 mW/cm^2. The performance of single direct ethanol fuel cell has no obvious improvement when Pt/C is replaced with Pt_1Pd_1/C as anode catalyst, and the two single cells have similar current density–voltage (*I–V*) curves. The single cell with Pt_1W_1/C as anode catalyst exhibits an improved performance compared to that with Pt/C and Pt_1Pd_1/C, respectively, especially in the intrinsic resistance-controlled region and mass transfer region. The maximum output power density is close to 16.0 mW/cm^2 at 90 °C. The single cell using either Pt_1Ru_1/C or Pt_1Sn_1/C exhibits superior performance to those with Pt/C, Pt_1Pd_1/C and Pt_1W_1/C. Both the OCV and the maximum power density increase when Pt_1Ru_1/C or Pt_1Sn_1/C is used. The OCV of single cell with Pt_1Ru_1/C is 0.67 V, about 0.12 V higher than that with Pt/C, and the maximum power density is 28.6 mW/cm^2 at 90 °C. When Pt_1Sn_1/C is adopted as the anode catalyst, the OCV of single fuel cell approaches to about 0.81 V, about 0.14 mV higher than the fuel cell with Pt_1Ru_1/C as anode catalyst. The maximum power density of the cell with Pt_1Sn_1/C is 52.0 mW/cm^2, nearly twice as that of the single cell with Pt_1Ru_1/C catalyst. The single cell results identify evidently that Pt_1Sn_1/C is more suitable to DEFC operated at 90 °C. On the other hand, in order to eliminate other factors influencing the performance of single cells, the single cells with PtSn and PtRu as anodes respectively were also evaluated further as half-cells. In the cathode, oxygen was replaced by the humidified hydrogen and the cathode was used as reference electrode and counter electrode. The anode was still fed with ethanol solution and used as working electrode. Fig. 5 is the anode polarization results of ethanol on PtRu and PtSn anode catalysts at 90 °C. From this figure, it is found that at the potential region less than 80 mV (versus DHE), the Pt_1Ru_1

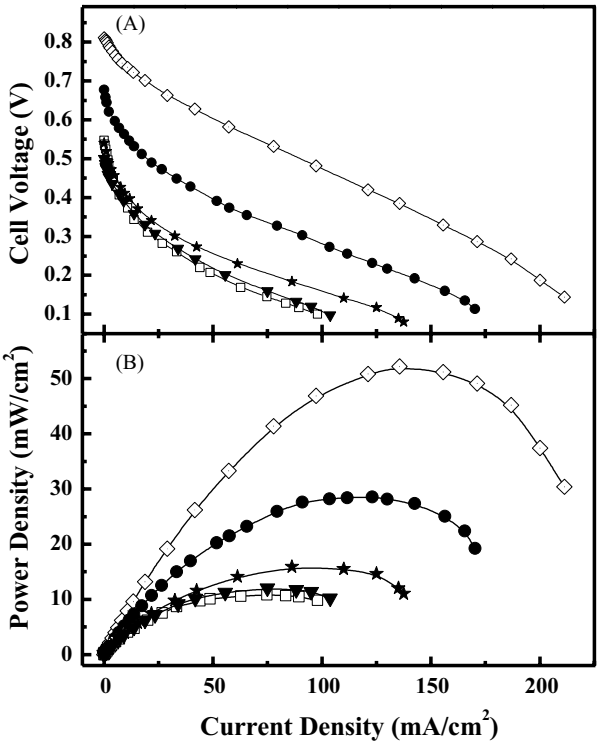

Fig. 4. Comparison of the fuel cell characteristics of a direct ethanol fuel cell with different anode catalysts operated at 90 °C; Anode catalyst and metal loading: (□) Pt/C, 2.0 mg Pt/cm^2; (▼) Pt_1Pd_1/C, 1.3 mg Pt/cm^2; (★) Pt_1W_1/C, 2.0 mg Pt/cm^2; (●) Pt_1Ru_1/C, 1.3 mg Pt/cm^2; (◇) Pt_1Sn_1/C, 1.3 mg Pt/cm^2; Nafion®-115 was used as electrolyte; Ethanol concentration and flow rate: 1 M and 1.0 ml/min; cathode catalyst and metal loading: 1.0 mg Pt/cm^2 (20 Pt%, Johnson Matthey Co.).

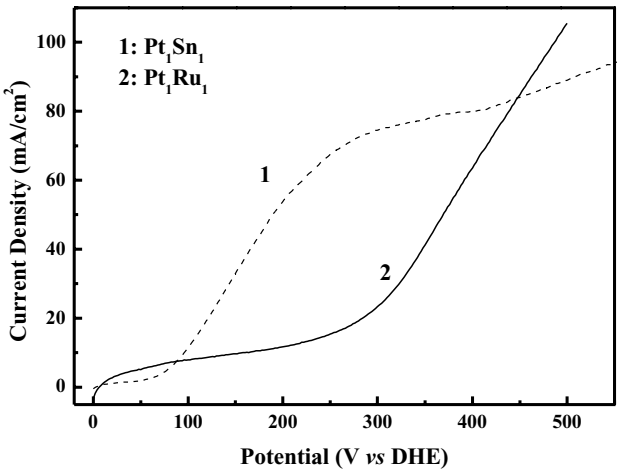

Fig. 5. The Ethanol anode polarization results of PtSn/C and PtRu/C at 90 °C. The cathode is supplied with 0.1 MPa (abs.) humidified (90 °C) H_2 at a flow rate of 40 ml/min. The anode is fed with 1.0 M ethanol solution at 1.0 ml/min. The scan rate is 2 mV/s.

catalyst shows more active than Pt_1Sn_1 toward ethanol electrooxidation at 90 °C. As the potential increases, the anode polarization current on Pt_1Sn_1 increases steeply from 85 mV (versus DHE). While the increment of the polarization current on Pt_1Ru_1 is very slow until the potential exceeds 300 mV (versus DHE). At 200 mV (versus DHE), the polarization current of ethanol on Pt_1Sn_1 is about 5 times that on Pt_1Ru_1. After 260 mV (versus DHE), the increment of the polarization current of ethanol oxidation on Pt_1Sn_1 also becomes slow. This result indicates that under the conditions of the single fuel cell operation, Pt_1Sn_1 is more active than Pt_1Ru_1 towards ethanol electro-oxidation, which is identical with the results of ethanol CV at RT and the single fuel cells.

Making alloys with a second or a third metal is a convenient way to modify the Pt electrocatalytic properties in order to increase the catalytic activity and weaken or even overcome poisoning by the methanol or ethanol electro-oxidation intermediates especially the adsorbed CO-like species. It is reported that Pt or PtRu catalytic activity to methanol electro-oxidation can be greatly improved when Pt or PtRu is modified with Mo or W [13–15]. The Mo (W) modified Pt or Pt_1Ru_1 catalysts should be used as anode catalysts for ethanol electro-oxidation considering the similar molecular structure of methanol and ethanol. In the present work, $Pt_1Ru_1W_1$/C, $Pt_1Ru_1Sn_1$/C and $Pt_1Ru_1Mo_1$/C catalysts were also prepared and used as anode catalysts for DEFC. The performances of single cells with Pt_1Ru_1/C, $Pt_1Ru_1Sn_1$/C, $Pt_1Ru_1W_1$/C and $Pt_1Ru_1Mo_1$/C respectively are showed in the Fig. 6. It is found that the performances of DEFCs are improved when $Pt_1Ru_1W_1$/C and $Pt_1Ru_1Mo_1$/C are used as anode catalysts in comparison with that single cell employing Pt_1Ru_1/C. The OCV of single cell with $Pt_1Ru_1Mo_1$/C increases to 0.72 V compared to 0.67 V of that with Pt_1Ru_1/C, while the *I–V* curve of single cell with $Pt_1Ru_1Mo_1$/C is close to that of single cell with Pt_1Ru_1/C. The OCV of single cell with $Pt_1Ru_1W_1$/C is about 0.7 V, higher than that with Pt_1Ru_1/C while less than that with $Pt_1Ru_1Mo_1$/C. The maximum power density of single cell with $Pt_1Ru_1W_1$/C is 38.5 mW/cm^2, 10 mW/cm^2 more than that of single cell with Pt_1Ru_1/C. But the performances of three single cells with ternary metallic catalysts are still less than that with Pt_1Sn_1/C. The single cell adopting $Pt_1Ru_1Sn_1$/C as anode catalyst also exhibits high performance as that with $Pt_1Ru_1W_1$/C, and the former is better than the latter in the intrinsic resistance-controlled region and activation-controlled region. XPS results indicated that Pt and Ru are in reduced state in all the carbon-supported Pt-based catalysts synthesized in the present work, while Sn is in oxidation state. It is also interesting to find from XRD result of Fig. 7 (here shown are only the simulated curves) that the lattice parameters of Pt_1Sn_1/C became shorter again after it has been modified by Ru, but still was longer than the lattice parameters of Pt/C and Pt_1Ru_1/C. The performance of the single fuel cell with $Pt_1Ru_1Sn_1$/C is coincidentally higher than that of the cell with Pt_1Ru_1/C,

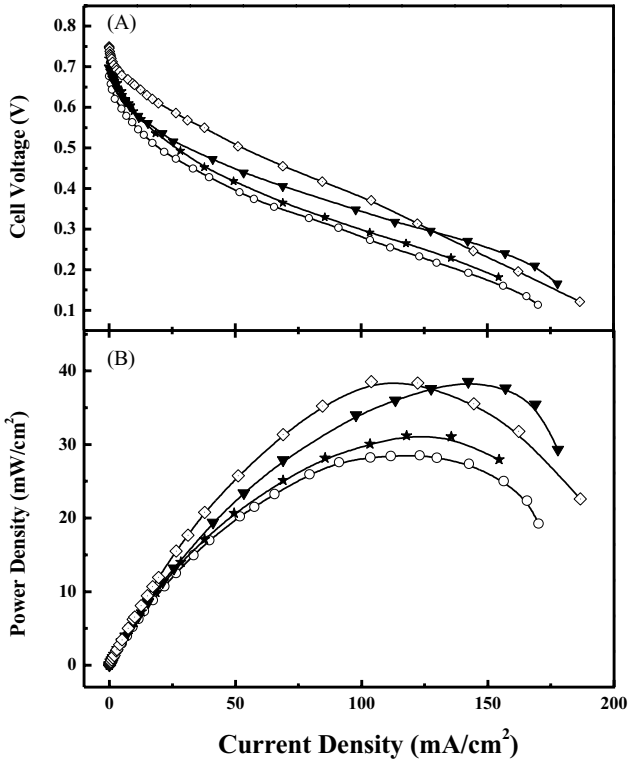

Fig. 6. Comparison of the fuel cell characteristics of a direct ethanol fuel cell with different anode catalysts operated at 90 °C, Anode catalyst: (○) Pt_1Ru_1/C; (▼) $Pt_1Ru_1W_1$/C; (★) $Pt_1Ru_1Mo_1$/C; (◇) $Pt_1Ru_1Sn_1$/C. The metal loading in anode is always 1.3 mg Pt/cm^2. Other conditions are the same as described for Fig. 4.

while still inferior to that of the cell with Pt_1Sn_1/C. Therefore, it is presumed from the above results that addition of Ru to Pt_1Sn_1/C is helpful to improve its conductivity, while it decreases its activity for ethanol electro-oxidation, one

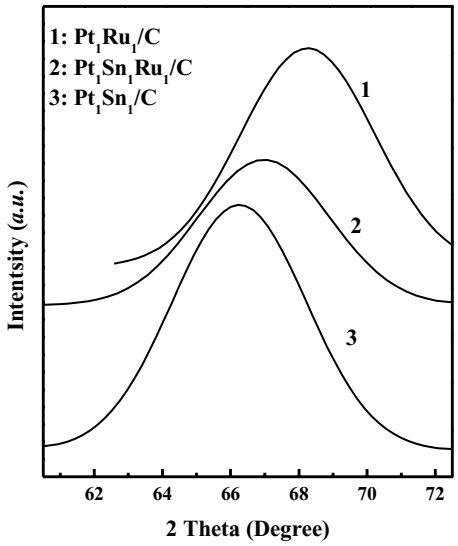

Fig. 7. The (2 2 0) diffraction peaks of carbon-supported Pt_1Sn_1, Pt_1Ru_1 and $Pt_1Sn_1Ru_1$.

reason for which is thought as the decrement of the lattice parameter.

CO-like intermediates are thought as the main poisoning species during electro-oxidations of ethanol and methanol. Thus how to oxidize CO-like intermediates as quickly as possible is very important to ethanol oxidation. As mentioned above, Pt and Ru are in metallic states and Sn of Pt_1Sn_1/C catalyst surfaces are in oxidation state. Ru and W have been demonstrated to easily provide $–OH_{ads}$ during methanol and ethanol oxidation [16], and the surface Sn or Sn oxides can also supply sufficient oxygen-containing species. Calculated binding energies [17] and experiment results [18] indicate that CO does not prefer to bind with Sn surface atoms, while CO can adsorb on Ru sites and some Ru surface active sites are probably not free for $–OH_{ads}$ formation [17]. Furthermore, Sn surface sites are always free to formation of $–OH_{ads}$ species, and oxygen-containing species prefers to adsorb on Sn than on Pt surface. Consequently, the Pt surface sites are free to ethanol adsorption and dehydrogenation. It is obvious that Sn (or Sn-oxide [19]), Ru and W are able to promote the formation of labile bonded oxygenated species at lower overpotentials than Pt. These oxygen-containing surface species are necessary for the oxidative removal of CO-like intermediates. This is the so-called bifunctional mechanism and explains the enhanced effect of Sn, Ru and W on the ethanol oxidation to a certain extent. But the enormous difference between single fuel cells performance with the bimetallic catalysts, PtSn/C and Pt_1Ru_1/C, could not be explained adequately in terms of bifunctional mechanism alone. The XRD and TEM results show that the particle size of Pt_1Ru_1/C is smaller than that of Pt_1Sn_1/C. As mentioned above, the lattice parameter of Pt_1Ru_1/C is less than that of Pt/C, while that of Pt_1Sn_1/C is larger than that of Pt/C. Thus, it is suggested that both the particle size effect and the interaction between Pt and Sn(Ru) play an important role in the ethanol electro-oxidation, especially the cleavage of C–C bond. The products distribution of direct ethanol fuel cells with PtRu and PtSn as anode catalysts shown that a relatively high ethanol conversion percent was found in the DEFC employing PtSn/C as anode [20]. CO_2 and acetic acid productivity of the DEFC with PtSn anode catalyst were higher than those of the DEFC with PtRu, indicating that PtSn is active toward both the ethanol electrooxidation and the C–C bond cleavage. More acetaldehyde was detected in the effluent solution of the DEFC with PtRu/C than that of the DEFC with PtSn/C. A very small amount of acetic ester was also detected in both effluents. The product distribution and ethanol conversion also indicated PtSn is more suitable for ethanol electro-oxidation than PtRu. More detailed study of mechanism of the enhanced ethanol oxidation reaction on Pt_1Sn_1/C catalyst is needed to carry out. Other two Pt-based bimetallic catalysts shown less activity than Pt_1Ru_1/C toward the ethanol oxidation, and their single fuel cell performances are also not better than those with Pt_1Ru_1/C and Pt_1Sn_1/C.

4. Conclusion

The TEM and XRD results demonstrate that nano-structure catalysts can be easily synthesized with the novel method, and the method is suitable to prepare supported Pt-based catalysts in the presence of higher metal loadings. There are different interactions between Pt and different addictives. In this present work, the results of the cyclic voltammetry test are coordinated with that of single fuel cell very well. Though thought as the best catalyst for methanol electro-oxidation in DMFCs at present, Pt_1Ru_1/C is not proved to be best anode catalyst for ethanol electro-oxidation. The addition of W and Mo can increase ethanol electro-oxidation activity on the Pt_1Ru_1/C catalyst. The *I–V* characteristics of single direct ethanol fuel cells show clearly that the Pt_1Sn_1/C is a better anode catalyst than Pt_1Ru_1/C and other carbon-supported bimetallic Pt-based catalysts for DEFCs. The single cell with $Pt_1Ru_1Sn_1$/C also shows an improved performance compared to the single cell with Pt_1Ru_1/C, but inferior to the performance with Pt_1Sn_1/C. From a practical point of view, Pt_1Sn_1/C is the better electrocatalyst for DEFCs among these anode catalysts investigated in the present work.

Acknowledgements

Authors would like to thank the “Greece–China Joint Research and Technology Programme 20003-2005” for funding. We also thank the financial support of National Natural Science Foundation of China (Grant No.: 20173060).

References

[1] B.D. McNicol, D.A.J. Rand, K.R. Williams, J. Power Sources 83 (1999) 15.
[2] H. Dohle, H. Schmitz, T. Bewer, et al., J. Power Sources 106 (2002) 313.
[3] X.M. Ren, P. Zelenay, S. Thomas, et al., J. Power Source 86 (2000) 111.
[4] S.C. Thomas, X.M. Ren, S. Gottsfeld, et al., Electrochim. Acta 47 (2002) 3741.
[5] T. Iwasita, E. Pastor, Electrochim. Acta 39 (1994) 531.
[6] B. Beden, M.-C. Morin, F. Hahn, et al., J. Electroanal. Chem. 229 (1987) 353.
[7] C. Lamy, E.M. Belgsir, J.-M. Léger, J. Appl. Electrochem. 31 (2001) 799.
[8] C. Yang, S. Srinivasan, A.S. Arico, P. Creti, et al., Electrochem. Solid State Lett. 4 (2001) A31.
[9] W. Zhou, Z. Zhou, S. Song, et al., Appl. Catal. B 46 (2003) 273.
[10] W.Z. Li, C.H. Liang, W.J. Zhou, et al., Carbon 1 (2002) 791.
[11] K. Scott, W. Taama, J. Power Sources 79 (1999) 43.
[12] V. Radmilovic, H.A. Gasteiger, et al., J. Catal. 154 (1995) 98.
[13] A.K. Shukla, M.K. Ravikumar, A.S. Arico, J. Appl. Electrochem. 25 (1995) 528.
[14] B.N. Grgur, G. Zhuang, M.M. Marvovich, et al., J. Phys. Chem. B 101 (1997) 3910.
[15] M. Götz, H. Wendt, Electrochim. Acta 43 (1998) 3637.

[16] A.B. Anderson, E. Grantscharova, S. Seong, J. Electrochem. Soc. 143 (1996) 2075.
[17] T.E. Shubina, M.T.M. Koper, Electrochimica Acta 47 (2002) 3621.
[18] A.N. Haner, P.N. Ross, U. Bardi, et al., J. Vac. Sci. Technol. A 10 (1992) 2718.
[19] T. Frelink, W. Visscher, J.A.R. Van Veen, Surf. Sci. 335 (1995) 353.
[20] W.J. Zhou, B. Zhou, W.Z. Li, Z.H. Zhou, S.Q. Song, G.Q. Sun, Q. Xin, S. Douvartzides, M. Goula, P. Tsiakaras, J. Power Sources 126 (2004) 16.